CrystEngComm

PAPER

View Article Online
View Journal | View Issue

Cite this: *CrystEngComm*, 2026, **28**, 2234

Synthesis of 2,7-dioctylbiphenylenodithiophenes for use as organic semiconducting materials in solution-processed organic thin-film transistors

Makoto Watanabe, *[a] Masato Miyashita,[a] Takashi Fukuda[b] and Shinya Oku[a]

Received 5th November 2025,
Accepted 2nd March 2026

DOI: 10.1039/d5ce01050k

rsc.li/crystengcomm

A synthetic route to 2,7-dialkylbiphenylenodithiophenes was developed and their potential as a new π-core system for organic semiconductors was investigated. The semiconductors 2,7-dioctylbiphenyleno[2,1-*b*:6,5-*b*′]dithiophene (**C8-B1-BPDT**), 2,7-dioctylbiphenyleno[1,2-*b*:5,6-*b*′]dithiophene (**C8-B2-BPDT**), and 2,7-dioctylbiphenyleno[2,3-*b*:6,7-*b*′]dithiophene (**C8-L-BPDT**) were synthesized from dihalobiphenylenes. Structural analysis by single-crystal X-ray crystallography revealed that **C8-B1-BPDT** adopts a herringbone motif whereas **C8-B2-BPDT** has an interdigitated structure. **C8-B1-BPDT** and **C8-B2-BPDT** displayed high solubilities of more than 0.80 wt% in toluene. In contrast, **C8-L-BPDT** exhibited a low solubility of 0.060 wt% in toluene at room temperature. Although **C8-B2-BPDT** formed noncontinuous films on a parylene-C dielectric layer by solution deposition, films of **C8-B1-BPDT** covered the whole area of the parylene-C layer. Bottom-contact bottom-gate thin-film transistors with a mobility of 0.58 $cm^2 V^{-1} s^{-1}$ were fabricated by drop casting of a solution of **C8-B1-BPDT**.

Introduction

Fused benzothiophene compounds have attracted considerable attention over the past few decades because of their use as semiconductor materials in organic thin-film transistors (OTFTs).[1–12] Solution-processable OTFT materials are attractive for healthcare monitoring systems because they enable the use of printing technologies such as inkjet printing to fabricate the organic semiconducting layer of OTFTs.[13,14] However, only a limited number of fused rigid benzothiophenes have yielded thin films with high mobility by solution deposition under ambient conditions.[2,7,9] These materials also require high thermal stability to withstand the heat during the device manufacturing process. Producing low-molecular-weight fused benzothiophene organic semiconductors with both high thermal stability and high solubility is still challenging.

Biphenylene is a fused rigid compound containing a four-membered ring and two benzene rings.[15] Biphenylene compounds are expected to have higher solubility than the corresponding anthracene compounds because of the smaller ring of the former compared with that of the latter. Therefore, here we focused on biphenylenodithiophene, which consists of a biphenylene and two thiophene rings, as a new π-core system.

Compounds with a biphenylene unit have not been used as semiconductor active layers for OTFTs to date. Only a few thiophene-fused biphenylenes have been reported and their synthetic methods are quite limited.[16,17] It is desirable to produce a wide range of biphenylenodithiophenes as potential semiconductor materials for OTFTs. Here we report the synthesis of three isomers of 2,7-dioctylbiphenylenodithiophene with centrosymmetry and their use in solution-processed OTFTs.

Results and discussion

Synthesis of biphenylenodithiophenes

The chemical structures of the three isomers are shown in Chart 1. The biphenylenodithiophene cores are denoted as **BPDT** with **B**- and **L**-indicating bent and linear cores, respectively. The selective syntheses of **C8-B1-BPDT**, **C8-B2-BPDT**, and **C8-L-BPDT** are shown in Scheme 1.

The synthetic methodology was first planned to consist of the syntheses of 2,6-difluorobiphenylene (**4**) and

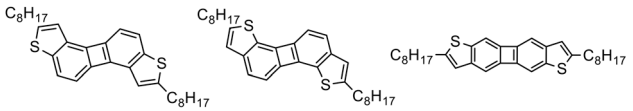

C8-B1-BPDT **C8-B2-BPDT** **C8-L-BPDT**

Chart 1 Molecular structures of three biphenylenodithiophene isomers.

[a] *Advanced Materials Research Laboratory, Tosoh Corporation, 2743-1 Hayakawa, Ayase-shi, Kanagawa 252-1123, Japan. E-mail: makoto-watanabe-zr@tosoh.co.jp*
[b] *Research and Development Planning, Tosoh Corporation, 2-2-1 Yaesu, Tyuou-ku, Tokyo 104-8467, Japan*

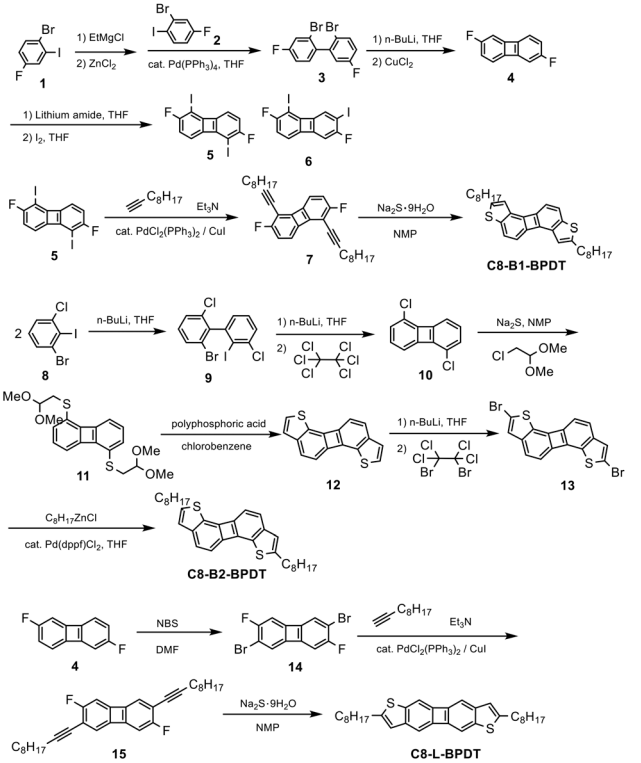

Scheme 1 Syntheses of **C8-B1-BPDT**, **C8-B2-BPDT**, and **C8-L-BPDT**.

1,5-dichlorobiphenylene (**10**), regioselective dihalogenation, chemoselective Sonogashira coupling reactions at the iodo or bromo sites, and ring closure with sodium sulfide. Biphenylene **4** was prepared by Negishi coupling of 1-bromo-4-fluorophenyl-2-zinc chloride derived from **1** with 2-bromo-4-fluoro-1-iodobenzene (**2**) to give **3**, followed by dilithiation of **3** with BuLi and $CuCl_2$-mediated oxidative cyclization to give **4**.[18] **4** is the intermediate for the synthesis of **C8-B1-BPDT** and **C8-L-BPDT**. We first carried out LDA[19]-mediated dilithiation of **4** followed by diiodination with iodine to afford a mixture of 2,6-difluoro-1,5-diiodobiphenylene (**5**) and an isomer **6** in a percentage ratio of 88% to 12%. It was found that the percentage ratio of **5** to **6** increased to 97% to 3% when lithium 2,2,6,6-tetramethylpiperidine (LTMP) was used instead of LDA. After purification by column chromatography and recrystallization, **5** was isolated. The symmetrical structure of **5** was confirmed by nuclear magnetic resonance (NMR) analyses (Fig. S15.5, SI). Sonogashira coupling of **5** with 1-decyne afforded **7**, which was cyclized with sodium sulfide[20,21] under mild reaction conditions to give 2,7-dioctylbiphenyleno[2,1-*b*:6,5-*b*′]dithiophene (**C8-B1-BPDT**) (Scheme 1).

The synthesis of the bent isomer 2,7-dioctylbiphenyleno[1,2-*b*:5,6-*b*′]dithiophene (**C8-B2-BPDT**) was also attempted by the same method starting with **10**, which was prepared by lithium-mediated homocoupling[22] of **8** *via* an aryne species followed by the lithium-mediated intramolecular cyclization[23] of **9** and quenching with hexachloroethane. Unfortunately, lithiation of **10** by lithium amide bases such as LDA followed by iodination gave only 1,5-dichloro-2-iodobiphenylene, and further lithiation and iodination resulted in the undesired formation of 1,5-difluoro-2,7-diiodobiphenylene. Therefore, a different route to synthesize **C8-B2-BPDT** was examined. In this alternative route, **10** was converted to 1,5-bis(2,2-dimethoxyethylthio)bipheneylene (**11**) in the presence of sodium sulfide and chloroacetaldehyde dimethyl acetal. Next, **11** was subjected to polyphosphoric acid-mediated cyclization[24] to give unsubstituted biphenyleno[1,2-*b*:5,6-*b*′] dithiophene (**12**). Dilithiation by BuLi at the 2- and 7-positions of the thiophene rings and bromination using 1,2-dibromotetrachloroethane afforded 2,7-dibromo compound **13**. Finally, **C8-B2-BPDT** was obtained by palladium-catalyzed coupling of **13** with octylzinc chloride.

The linear isomer **C8-L-BPDT** was synthesized following a similar process to that used to obtain **C8-B1-BPDT**. Electrophilic bromination of **4** using NBS selectively gave 2,6-dibromo-3,7-difluorobiphenylene (**14**) in moderate yield. The symmetry of **14** was also confirmed by NMR analysis (Fig. S15.23, SI). Sonogashira coupling of **14** with 1-decyne and cyclization using sodium sulfide gave 2,7-dioctylbiphenyleno[2,3-*b*:6,7-*b*′]dithiophene (**C8-L-BPDT**).

All the new materials were fully characterized by spectroscopic analyses including NMR and mass spectrometry (MS). Furthermore, single-crystal X-ray analyses of **C8-B1-BPDT** and **C8-B2-BPDT** confirmed the structure of the dialkylbiphenylenodithiophene framework (*vide infra*).

Properties of biphenylenodithiophenes

The solubilities of bent **C8-B1-BPDT** and **C8-B2-BPDT** in toluene were as high as 1.6 and 0.80 wt%, respectively, at ambient temperature. Thus, drop casting of these solutions was able to be carried out under ambient conditions. High solubility is one of the requisite factors to realize printed electronics. Printing techniques such as inkjet printing are usually conducted under ambient conditions. A solution of **C8-B1-BPDT** in toluene formed a continuous film on a parylene-C layer by drop casting, whereas a crystalline precipitate with a dendrite-like morphology was obtained by drop casting of a solution of **C8-B2-BPDT**. Drop casting of a toluene solution of the linear isomer **C8-L-BPDT** resulted in precipitation of solid **C8-L-BPDT** because its solubility in toluene was only 0.060 wt% under ambient conditions. Thus, a thin film of **C8-L-BPDT** was fabricated by vacuum deposition. Fig. S1 (SI) exhibits laser microscope images of thin films of **C8-B1-BPDT** and **C8-B2-BPDT** obtained by drop casting a toluene solution on the surface of a parylene-C layer insulator film. The thin film morphology was also examined by scanning electron microscope (SEM) (Fig. S3 and S5, SI) and atomic force microscope (AFM) (Fig. S4 and S5, SI).

Ultraviolet–visible (UV–vis) spectra of **C8-B1-BPDT** in dichloromethane solution and a thin film are presented in Fig. 1. UV–vis spectra of **C8-B2-BPDT** and **C8-L1-BPDT** in dichloromethane are shown in Fig. S6 (SI). The optical highest occupied molecular orbital (HOMO)–lowest

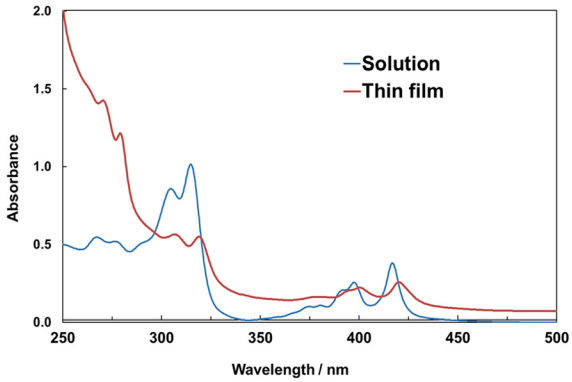

Fig. 1 UV–vis spectra of **C8-B1-BPDT** in dichloromethane solution and a thin film.

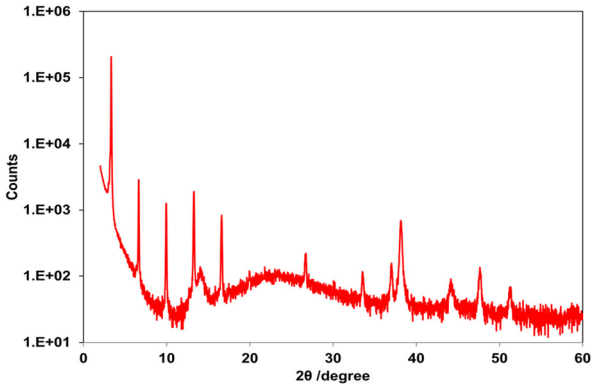

Fig. 3 Out-of-plane XRD profile of a drop-cast thin film of **C8-B1-BPDT**.

unoccupied molecular orbital (LUMO) gap of the thin film of **C8-B1-BPDT** estimated from the absorption edge (λ_{edge} = 427 nm) was about 2.9 eV.

The ionization potentials (IPs) of the biphenylenodithiophenes were estimated using photoelectron spectroscopy in air. Estimated IPs of thin films of **C8-B1-BPDT** and **C8-L-BPDT** were 5.2 and 5.7 eV, respectively (Fig. S7, SI). It is assumed that the smaller IP for **C8-B1-BPDT** than that of **C8-L-BPDT** may imply that the former has a more closely packed molecular arrangement than the latter, arising from molecular packing and intermolecular interactions.[25] Judging from its HOMO–LUMO gap and IP, **C8-B1-BPDT** is expected to be electrochemically stable (Fig. S12, SI).

Differential scanning calorimetry (DSC) measurements revealed that **C8-B1-BPDT** had a melting point of 140 °C without any phase rearrangement (Fig. 2), whereas **C8-B2-BPDT** had a relatively low melting point of 107 °C (Fig. S8.1, SI) and linear **C8-L-BPDT** had a high melting point of 285 °C without any phase rearrangement (Fig. S8.2, SI). Thus, **C8-B1-BPDT** was found to have both high solubility in toluene and a high melting point.

Fig. 3 and S9.1 and S9.2 (SI) show out-of-plane X-ray diffraction (XRD) patterns of drop-cast thin films of **C8-B1-BPDT** and **C8-B2-BPDT** and a vacuum-deposited thin film of **C8-L-BPDT** on parylene-C fabricated at ambient temperature, respectively. **C8-B1-BPDT** adopted a layered structure and exhibited a series of peaks assignable to multiple (00*l*) diffractions, meaning that the molecules were aligned perpendicular to the substrate. The interlayer distance (*d*-spacing) was calculated to be 26.6 Å from these reflections, which is almost half the crystallographic *c*-axis of its bulk single crystal and its molecular length (*vide infra*). In contrast, the diffraction pattern of **C8-B2-BPDT** displayed only a weak peak corresponding to 10.0 Å, meaning that the molecules were not oriented perpendicular to the substrate. The **C8-L-BPDT** thin film displayed weak peaks assignable to (001) and (004) diffractions and the interlayer distance (*d*-spacing) was calculated to be 31.8 Å.

In-plane reciprocal lattice mapping measurements were carried out for the drop-cast thin film of **C8-B1-BPDT** (Fig. 4a). The XRD profiles collected by scanning the φ angle (0–360°) were integrated and converted to a linear $2\theta\chi$ scan pattern (Fig. 4b). The peak at 16.2° (*d*-spacing of 5.5 Å) was assigned to the (200) diffraction of the single-crystal lattice, which is almost half the crystallographic *a*-axis (10.9 Å) of its bulk single crystal (*vide infra*).

Single crystals suitable for X-ray structural analysis were obtained for **C8-B1-BPDT** and **C8-B2-BPDT**. The single crystal of **C8-B1-BPDT** belonged to the monoclinic *I*2/*a* space group with two molecules along the *c*-axis in the unit cell. The

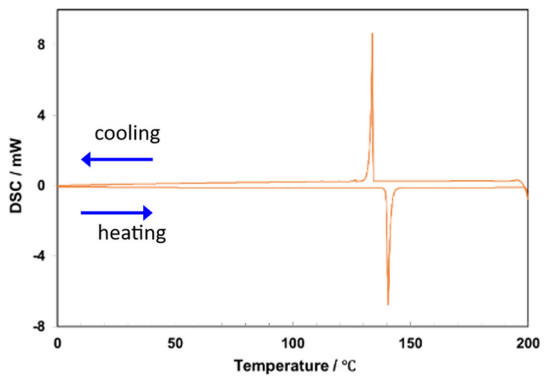

Fig. 2 DSC curves of **C8-B1-BPDT**. The scan rate was 10 °C min^{-1}.

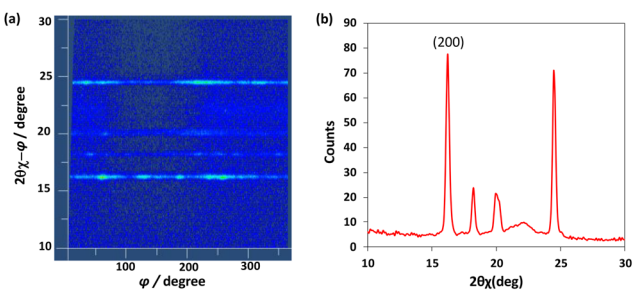

Fig. 4 In-plane XRD analysis of a drop cast thin film of **C8-B1-BPDT** (incident angle, 0.20°). (a) In-plane reciprocal lattice mapping and (b) in-plane XRD profile.

molecules were arranged with herringbone packing, which enables two-dimensional carrier transport, and the alkyl moieties were located above and below the core plane (Fig. 5). In contrast, **C8-B2-BPDT** crystallized in the monoclinic *P*1 space group. The XRD analysis unveiled an interdigitated arrangement, which is unfavorable for carrier transport, and the alkyl moieties were located on the same plane as the core (Fig. S10, SI). Crystallographic parameters were summarized in Table S1 (SI).

OTFT devices with biphenylenodithiophenes

Bottom-contact bottom-gate OTFT devices were fabricated using a solution process to form semiconducting layers of **C8-B1-BPDT** and **C8-B2-BPDT**. Silver was thermally deposited as the gate electrodes on a glass substrate, and then a parylene-C dielectric layer was deposited by chemical vapor deposition. Gold was vacuum deposited through a shadow mask as the source–drain electrodes, which were treated with PFBT to give a channel length and width of 100 and 500 μm, respectively. Finally, a toluene solution of organic semiconductor material was drop cast to complete fabrication of OTFT devices. **C8-B1-BPDT** covered the source–drain electrodes to give a crystalline thin film, whereas **C8-B2-BPDT** formed a noncontinuous film that partially covered the source–drain electrodes (Fig. S1, SI). Because of its poor solubility, **C8-L-BPDT** was vacuum deposited on the source–drain electrodes at ambient substrate temperature. These devices were evaluated under ambient conditions and showed typical p-channel responses. The field-effect mobilities were extracted from the saturation regime. The characteristics of the OTFTs are summarized in Table 1. **C8-B1-BPDT**-based devices exhibited a mobility of 0.21 $cm^2\ V^{-1}\ s^{-1}$ (Fig. S13, SI). Their mobility was increased up to 0.58 $cm^2\ V^{-1}\ s^{-1}$ with an I_{on}/I_{off} ratio of 4.6×10^7 using a polystyrene (PS) blend formulation (Fig. 6). It is assumed that vertical phase separation[26] between the organic semiconductor and insulating polymer gave rise to this mobility increase. That is, PS could fill voids in the interface between **C8-B1-BPDT**, the dielectric and the source–drain electrodes in a bottom-gate bottom-contact device and afford smoother underlayer to **C8-B1-BPDT** than the absence of PS. In the presence of PS, interface trap density (D_{it}) values were found to decrease (Table S2, SI). The morphology of a drop-cast thin film of **C8-B1-BPDT** with PS was observed by SEM and AFM (Fig. S5, SI).

Structurally comparable NDT[3,27] and ADT[5,28–33] compounds without a triethylsilylethynyl moiety did not show field-effect activity after solution deposition except for linear dihexylADT[34] and bent monosubstituted ADT compounds.[35] The bent isomer **C8-B2-BPDT** and linear **C8-L-BPDT** showed lower mobilities of 10^{-4} and 10^{-3} $cm^2\ V^{-1}\ s^{-1}$, respectively (Fig. S11, SI). Spin coating methods were also examined for those three compounds. A solution of **C8-B1-BPDT** gave mobilities of 0.073 $cm^2\ V^{-1}\ s^{-1}$ without PS and 0.12 $cm^2\ V^{-1}\ s^{-1}$ with PS, respectively (Table 1 and Fig. S14, SI). On the other hand, continuous films that covered the source–drain electrodes were obtained from **C8-B2-BPDT** and **C8-L-BPDT** but both showed no transistor performance with or without PS. Fig. S2 (SI) exhibits a laser microscope image of thin films of these three compounds with PS obtained by spin coating.

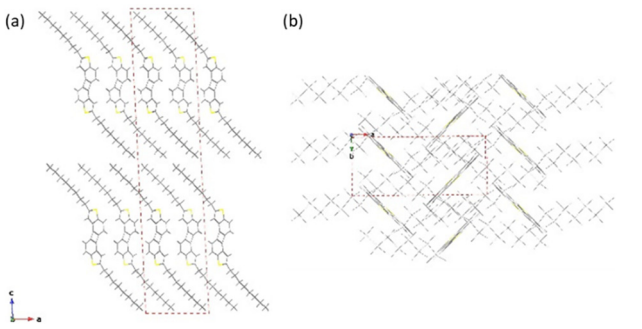

Fig. 5 Crystal structure of **C8-B1-BPDT**. (a) *b*-Axis projection showing a layer-by-layer arrangement and (b) *c*-axis projection.

Conclusions

A series of dialkylbiphenylenodithiophene compounds was synthesized and their use as organic semiconductor materials in OTFTs was explored. The straightforward synthetic route enabled the synthesis of a variety of bent and linear isomers of biphenylenodithiophene with different substituents. The bent core systems with biphenyleno[2,1-*b*:6,5-*b*′]dithiophene and biphenyleno[1,2-*b*:5,6-*b*′]dithiophene exhibited high solubility in toluene at ambient temperature, making them promising core systems for device fabrication using printing technology. In particular, **C8-B1-BPDT** formed continuous films by drop casting that showed a carrier mobility as high as 0.58 $cm^2\ V^{-1}\ s^{-1}$. We will investigate this core system with different substituents as semiconductor materials for OTFTs in the future.

Experimental

Synthesis of compounds

General. All chemicals and solvents were of reagent grade unless otherwise indicated. Anhydrous-grade tetrahydrofuran (THF), *N*-methylpyrrolidone (NMP), and chlorobenzene were used as received. All reactions were carried out under nitrogen atmosphere. Silica gel used in chromatographic separations was obtained from Fujifilm Wako Pure Chemical Corp. (Wakogel® 60N, 38–100 μm). NMR spectra were measured with a JEOL Delta spectrometer at 400 MHz. Chemical shifts are reported in parts per million (ppm, δ scale) from residual protons in the deuterated solvent for ^{1}H NMR spectra (δ 7.26 ppm for chloroform) and from the solvent carbon for ^{13}C NMR spectra (δ 77.16 ppm for chloroform). MS were measured on a gas chromatograph-mass spectrometer (Shimadzu QP2010SE) by an electron impact ionization procedure (70 eV) or a liquid

Table 1 OTFT performance of 2,7-dioctylbiphenylenodithiophenes

Compound	Deposition method	Mobility[a] ($cm^2\ V^{-1}\ s^{-1}$)	I_{on}/I_{off}	V_{th} (V)
C8-B1-BPDT	Drop casting[b]	0.21	1.0×10^{-7}	−1.0
C8-B1-BPDT[c]	Drop casting[b]	0.58	4.6×10^{-7}	−2.9
C8-B2-BPDT	Drop casting[b]	0.0002	1.0×10^{-3}	−0.9
C8-L-BPDT	Vacuum deposition[d]	0.004	1.0×10^{-4}	−10.3
C8-B1-BPDT	Spin coating[e]	0.073	1.0×10^{-5}	−1.2
C8-B1-BPDT[c]	Spin coating[e]	0.12	2.4×10^{-5}	−2.6

[a] Extracted from the saturation regime (V_{DS} = −20 V). [b] 0.2 wt% of the compound in toluene was used. [c] 0.05 wt% of polystyrene (M_W = 280 000) was included. [d] The substrate was maintained at room temperature. [e] 0.4 wt% of the compound in toluene was spin-coated at 2000 rpm for 40 s.

chromatograph-mass spectrometer (Bruker microTOF) by an atmospheric-pressure chemical ionization (APCI) procedure. High-resolution mass spectrometry (HRMS) was carried out on a JEOL JMS-700 MStation spectrometer.

2,2′-Dibromo-4,5′-difluoro-1,1′-biphenyl (3). EtMgBr (2.0 M in THF, 11.4 mL, 22.8 mmol) was added to a solution of 1-bromo-4-fluoro-2-iodobenzene (**1**, 6.67 g, 22.2 mmol) in THF (25 mL) at 0 °C and stirred at 0 °C for 15 min. Subsequently, this solution was introduced to a solution of zinc chloride (4.26 g, 31.3 mmol) in THF (28 mL) *via* cannula at 0 °C and stirred at 0 °C for 15 min. After the resulting white suspension was allowed to warm to room temperature, 2-bromo-4-fluoro-1-iodobenzene (**2**, 5.44 g, 18.1 mmol) and $Pd(PPh_3)_4$ (155 mg, 0.134 mmol, 0.74 mol%) were added and then the mixture was stirred at 50 °C for 4 h. After addition of 1 N HCl to the ice-cold mixture, the organic layer was extracted with hexane, washed with water, dried over Na_2SO_4, and concentrated *in vacuo*. The residue was purified by column chromatography on silica gel (hexane) to afford 2,2′-dibromo-4,5′-difluoro-1,1′-biphenyl (**3**, 5.94, g, 17.0 mmol, 93%) as a colorless oil. ^{1}H NMR (400 MHz, $CDCl_3$): δ 6.95–7.04 (m, 2H), 7.11 (dt, J = 8.6 Hz, J = 2.7 Hz, 1H), 7.21 (dd, J = 8.6 Hz, J = 5.9 Hz, 1H), 7.42 (dd, J = 8.3 Hz, J = 2.6 Hz, 1H), 7.62 (dd, J = 8.7 Hz, J = 5.2 Hz, 1H); ^{13}C NMR (100 MHz, $CDCl_3$): δ 114.71 (d, J = 21.2 Hz, CH), 117.01 (d, J = 22.2 Hz, CH), 118.23 (C_{quat}), 118.50 (d, J = 22.8 Hz, CH), 120.13 (d, J = 20.3 Hz, CH), 123.60 (d, J = 9.5 Hz, C_{quat}), 131.83 (d, J = 8.4 Hz, CH), 134.03 (d, J = 8.1 Hz, CH), 137.33 (C_{quat}), 142.77 (d, J = 8.3 Hz, C_{quat}), 161.61 (d, J = 246.7 Hz, C_{quat}), 162.19 (d, J = 250.8 Hz, C_{quat}).

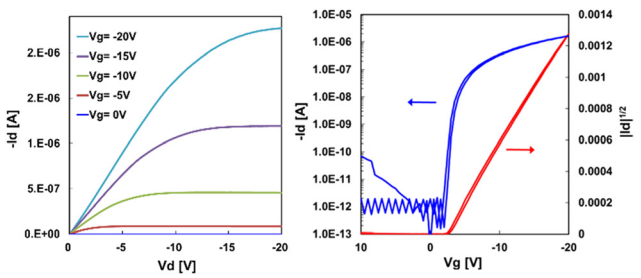

Fig. 6 Typical characteristics of OTFTs with drop-cast **C8-B1-BPDT** layers: output characteristics (left) and transfer characteristics at V_d = −20 V (right).

2,6-Difluorobiphenylene (4). *n*-BuLi (22.5 mL, 1.6 M in hexane, 36.0 mmol) was added dropwise to a solution of 2,2′-dibromo-4,5′-difluoro-1,1′-biphenyl (**3**, 5.84 g, 16.8 mmol) in THF (250 mL) at −78 °C. After stirring for 1 h at −78 °C, anhydrous $CuCl_2$ (6.35 g, 47.3 mmol) was added in one portion and the resulting mixture was gradually allowed to warm to room temperature. The reaction was quenched with 6 N HCl and then the organic layer was extracted with hexane, washed with brine and water, dried over Na_2SO_4, and concentrated *in vacuo*. The residue was purified by column chromatography on silica gel (hexane) followed by recrystallization from ethanol to afford 2,6-difluorobiphenylene (**4**, 1.82 g, 9.69 mmol, 58%) as a pale yellow solid. Mp 111.5–112.4 °C; ^{1}H NMR (400 MHz, $CDCl_3$): δ 6.38 (m, 2H), 6.40 (d, J = 7.2 Hz, 2H), 6.56 (dd, J = 7.7 Hz, J = 4.2 Hz, 2H); ^{13}C NMR (100 MHz, $CDCl_3$): δ 107.94 (d, J = 27.4 Hz, CH), 112.78 (d, J = 24.7 Hz, CH), 118.87 (d, J = 8.9 Hz, CH), 143.50 (C_{quat}), 152.44 (d, J = 9.1 Hz, C_{quat}), 163.66 (d, J = 247.0 Hz, C_{quat}).

2,6-Difluoro-1,5-diiodobiphenylene (5). *n*-BuLi (11.8 mL, 1.6 M in hexane, 18.9 mmol) was added to a solution of 2,2,6,6-tetramethylpiperidine (2.72 g, 19.2 mmol) in THF (50 mL) at −55 °C and then the resulting solution was stirred for 30 min at −55 °C to form LTMP. A solution of 2,6-difluorobiphenylene (**4**, 1.42 g, 7.54 mmol) in THF (25 mL) was added dropwise to the solution of LTMP at −78 °C. After stirring for 1 h at −78 °C, the reaction was quenched with a solution of iodine (4.71 g, 18.6 mmol) in THF (30 mL) and then the mixture was allowed to warm to room temperature. After addition of brine, the resulting mixture was extracted with toluene, washed with a dilute solution of Na_2SO_3 and water, dried over Na_2SO_4, and concentrated *in vacuo*. The residue was purified by column chromatography on silica gel (hexane) followed by recrystallization from toluene : heptane (2 : 1) to afford 2,6-difluoro-1,5-diiodobiphenylene (**5**, 2.30 g, 5.22 mmol, 69%) as a pale yellow solid. Mp 197.0–198.5 °C; ^{1}H NMR (400 MHz, $CDCl_3$): δ 6.43 (dd, J = 9.6 Hz, J = 7.3 Hz, 2H), 6.68 (dd, J = 7.2 Hz, J = 4.0 Hz, 2H); ^{13}C NMR (100 MHz, $CDCl_3$): δ 71.70 (d, J = 31.1 Hz, C_{quat}), 113.26 (d, J = 26.8 Hz, CH), 117.41 (d, J = 7.9 Hz, CH), 144.98 (C_{quat}), 156.57 (d, J = 1.8 Hz, C_{quat}), 162.24 (d, J = 249.1 Hz, C_{quat}).

1,5-Di(dec-1-yn-1-yl)-2,6-difluorobiphenylene (7). 1-Decyne (270 mg, 1.95 mmol) was added to a solution of 2,6-difluoro-1,5-diiodobiphenylene (**5**, 284 mg, 0.647 mmol), triethylamine (5.0 mL), $Pd(PPh_3)_2Cl_2$ (11.0 mg, 0.0156 mmol, 2.4 mol%), and CuI (6.3 mg, 0.033 mmol, 5.1 mol%) in toluene (3 mL). After the mixture was stirred for 20 h at room temperature, 1 N HCl was added at 0 °C. The resulting mixture was extracted with toluene and then the organic layer was washed with water, dried over Na_2SO_4, and concentrated *in vacuo*. The residue was purified by column chromatography on silica gel eluted with hexane to give 1,5-di(dec-1-yn-1-yl)-2,6-difluorobiphenylene (**7**, 208 mg, 0.451 mmol, 70%) as a pale yellow solid. Mp 60.8–61.3 °C; ^{1}H NMR (400 MHz, $CDCl_3$): δ 0.89 (t, J = 6.6 Hz, 6H), 1.30 (m, 16H), 1.45 (m, 4H), 1.60 (m, 4H), 2.44 (t, J = 7.1 Hz, 4H), 6.40 (dd, J = 11.1 Hz, J = 7.4 Hz, 2H), 6.54 (dd, J = 7.3 Hz, J = 4.0 Hz, 2H); ^{13}C NMR (100 MHz, $CDCl_3$): δ 14.27, 19.84, 22.83, 28.65, 28.99, 29.25, 29.38, 31.99, 70.74 (C_{quat}), 98.64 (C_{quat}), 105.78 (d, J = 22.4 Hz, C_{quat}), 112.86 (d, J = 24.7 Hz, CH), 117.86 (d, J = 8.3 Hz, CH), 142.51 (C_{quat}), 153.02 (C_{quat}), 162.82 (d, J = 252.4 Hz, C_{quat}). HRMS (DART): calcd for $C_{32}H_{39}F_2$ $[M + H]^+$ 461.3014, found, 461.3016.

2,7-Dioctylbiphenyleno[2,1-*b*:6,5-*b*′]dithiophene (C8-B1-BPDT). NMP (3 mL) was added to a mixture of 1,5-di(dec-1-yn-1-yl)-2,6-difluorobiphenylene (**7**, 78.3 mg, 0.169 mmol) and sodium sulfide nonahydrate (124 mg, 0.517 mmol), and then the resulting mixture was heated at 70 °C for 6 h. After cooling to 0 °C, the resulting mixture was quenched with water, extracted with toluene, washed with brine, dried over Na_2SO_4, and concentrated *in vacuo*. The residue was purified by column chromatography on silica gel (hexane) followed by recrystallization from heptane to give 2,7-dioctylbiphenyleno[2,1-*b*:6,5-*b*′]dithiophenes (**C8-B1-BPDT**, 45.0 mg, 0.0920 mmol, 54%) as yellow plates. Mp 140.3–140.8 °C; ^{1}H NMR (400 MHz, $CDCl_3$): δ 0.89 (t, J = 6.8 Hz, 6H), 1.25–1.40 (m, 20H), 1.70 (m, 4H), 2.78 (t, J = 7.2 Hz, 4H), 6.54 (d, J = 7.5 Hz, 2H), 6.60 (s, 2H), 7.04 (d, J = 7.4 Hz, 2H); ^{13}C NMR (100 MHz, $CDCl_3$): δ 14.28, 22.83, 29.28, 29.36, 29.49, 30.74, 31.17, 32.02, 112.97, 116.35, 120.34, 131.41, 141.34, 144.92, 148.16, 149.88; TOF HRMS (APCI): calcd for $C_{32}H_{41}S_2$ $[M + H]^+$ 489.2644, found, 489.2681.

2-Bromo-3′,6-dichloro-2′-iodobiphenyl (9). This compound could not be isolated by the literature method[22] because of its low selectivity. An investigation of the reaction conditions enabled us to synthesize **9** as follows. *n*-BuLi (18.8 mL, 1.6 M in hexane, 30.0 mmol) was added to a solution of 1-bromo-3-chloro-2-iodobenzene (**8**, 16.4 g, 51.8 mmol) in THF (95 mL) at −78 °C and then the resulting solution was stirred for 30 min at −78 °C. The cooling bath was removed and the reaction vessel was immediately placed in a water bath at 30 °C and stirred for 30 min at 30 °C. After addition of water at room temperature, the resulting mixture was extracted with hexane, washed with water, dried over Na_2SO_4, and concentrated *in vacuo*. The residue was washed with ethanol to afford 2-bromo-3′,6-dichloro-2′-iodobiphenyl (**9**, 7.21 g, 16.8 mmol, 65%) as a white solid. Mp 145–146 °C; ^{1}H NMR (400 MHz, $CDCl_3$): δ 7.03 (dd, J = 7.8 Hz, J = 1.4 Hz, 1H), 7.23 (t, J = 7.8 Hz, 1H), 7.39 (t, J = 7.8 Hz, 1H), 7.46 (dd, J = 8.2 Hz, J = 1.3 Hz, 1H), 7.50 (dd, J = 8.2 Hz, J = 1.4 Hz, 1H), 7.61 (dd, J = 8.0 Hz, J = 1.2 Hz, 1H); ^{13}C NMR (100 MHz, $CDCl_3$): δ 103.89, 124.81, 127.76, 128.78, 128.90, 129.56, 130.38, 131.34, 134.75, 139.75, 143.78, 147.14.

1,5-Dichlorobiphenylene (10). *n*-BuLi (26.0 mL, 1.6 M in hexane, 41.6 mmol) was added to a solution of 2-bromo-3′,6-dichloro-2′-iodobiphenyl (**9**, 5.07 g, 11.8 mmol) in THF (100 mL) at −78 °C and then the resulting solution was stirred for 40 min at −78 to −74 °C. A solution of hexachloroethane (5.55 g, 23.4 mmol) in THF (10 mL) at −78 °C was added to the reaction mixture. The resulting mixture was allowed to warm to room temperature. After addition of brine, the mixture was extracted with hexane, washed with brine and water, dried over Na_2SO_4, and concentrated *in vacuo*. The residue was purified by recrystallization from ethanol to afford 1,5-dichlorobiphenylene (**10**, 1.64 g, 7.43 mmol, 63%) as a pale yellow solid. Mp 122.6–122.9 °C; ^{1}H NMR (400 MHz, $CDCl_3$): δ 6.64 (d, J = 6.2 Hz, 2H), 6.70 (d, J = 8.4 Hz, 2H), 6.75 (dd, J = 8.7 Hz, J = 6.4 Hz, 2H); ^{13}C NMR (100 MHz, $CDCl_3$): δ 116.41, 123.12, 129.82, 130.76, 146.54, 150.10.

1,5-Bis((2,2-dimethoxyethy)thio)biphenylene (11). Chloroacetaldehyde dimethyl acetal (2.37 g, 19.0 mmol) was added to a mixture of sodium sulfide nonahydrate (3.00 g, 12.4 mmol) in *N*-methylpyrrolidone (38 mL). The resulting solution was stirred for 20 min at room temperature. To the resulting solution was added 1,5-dichlorobiphenylene (**10**, 703 mg, 3.18 mmol) and then the mixture was warmed to 120 °C. After stirring for 3 h at 120 °C, chloroacetaldehyde dimethyl acetal (1.10 g, 8.83 mmol) and sodium sulfide nonahydrate (2.13 g, 8.87 mmol) were added and then the mixture was stirred for a further 3 h at 120 °C. The addition of chloroacetaldehyde dimethyl acetal and sodium sulfide nonahydrate and heating process were repeated three further times. After cooling, the reaction mixture was quenched with water, extracted with toluene, washed with water, dried over Na_2SO_4, and concentrated *in vacuo*. The byproduct bis(2,2-dimethoxyethyl)sulfane was removed by distillation under reduced pressure (120 Pa). The residue was purified by column chromatography on silica gel (toluene : ethyl acetate = 20 : 1) to afford 1,5-bis((2,2-dimethoxyethy)thio)biphenylene (**11**) (886 mg, 2.26 mmol, 71%) as an amber viscous oil; ^{1}H NMR (400 MHz, $CDCl_3$): δ 3.10 (d, J = 5.8 Hz, 4H), 3.38 (s, 12H), 4.53 (t, J = 5.6 Hz, 2H), 6.54 (dd, J = 5.8 Hz, J = 1.8 Hz, 2H), 6.66–6.74 (m, 4H); ^{13}C NMR (100 MHz, $CDCl_3$): δ 35.37, 53.91, 103.29, 115.95, 126.65, 129.53, 148.64, 150.76.

Biphenyleno[1,2-*b*:5,6-*b*′]dithiophene (12). Chlorobenzene (44 mL) was placed in a 300 mL flask equipped with two dropping funnels and vigorously stirred at 130 °C. PPA (7.56 g) and a solution of **11** (1.60 g, 4.09 mmol), triethylamine (0.74 g, 7.3 mmol), and chlorobenzene (20 mL) were placed in the first and second dropping funnels, respectively, and added dropwise over 3 h at 130 °C with vigorous stirring. The resulting mixture was stirred at 130 °C

for 6 h, cooled to room temperature, and then filtered. The black residue was washed with toluene twice and filtered. The resulting filtrate was combined and concentrated *in vacuo*. The residue was purified by column chromatography on silica gel (toluene) and washed with hexane to afford biphenyleno[1,2-*b*:5,6-*b*′] dithiophene (**12**, 591 mg, 2.23 mmol, 55%) as a reddish solid. Mp 197.1–197.8 °C; ^{1}H NMR (400 MHz, $CDCl_3$): δ 6.72 (d, J = 7.6 Hz, 2H), 7.03 (d, J = 5.5 Hz, 2H), 7.19 (d, J = 5.5 Hz, 2H), 7.20 (d, J = 7.4 Hz, 2H); ^{13}C NMR (100 MHz, $CDCl_3$): δ 114.21, 123.24, 124.59, 126.87, 128.26, 143.00, 145.44, 146.61.

2,7-Dibromobiphenyleno[1,2-*b*:5,6-*b*′]dithiophene (13). To a solution of **12** (138 mg, 0.525 mmol) in THF (14 mL) at −78 °C was added *n*-BuLi (1.2 mL, 1.6 M in hexane, 1.9 mmol). The resulting solution was stirred for 10 min at −78 °C followed by 20 min at room temperature. After cooling at −78 °C again, the reaction was quenched with a solution of 1,2-dibromo-1,1,2,2-tetrachloroethane (593 mg, 1.82 mmol) in THF (6 mL) and then the whole mixture was allowed to warm to room temperature. After addition of water, the resulting mixture was concentrated *in vacuo* to remove THF. The orange suspension was filtered and then washed sequentially with water, methanol, and hexane to afford 2,7-dibromobiphenyleno[1,2-*b*:5,6-*b*′]dithiophene (**13**, 184 mg, 0.436 mmol, 83%) as an orange solid. Mp >250 °C; ^{1}H NMR (400 MHz, $CDCl_3$, 58 °C): δ 6.64 (d, J = 7.4 Hz, 2H), 7.05 (s, 2H), 7.07 (d, J = 7.4 Hz, 2H); ^{13}C NMR (100 MHz, $CDCl_3$, 58 °C): δ 114.91, 116.75, 122.50, 127.38, 129.60, 142.81, 144.18, 146.19.

2,7-Dioctylbiphenyleno[1,2-*b*:5,6-*b*′]dithiophene (C8-B2-BPDT). Octylmagnesium chloride (2.0 M in THF, 0.40 mL, 0.80 mmol) was added to a solution of zinc chloride (177 mg, 1.29 mmol) in THF (5 mL) at 0 °C. The resulting solution was stirred for 15 min at 0 °C followed by 20 min at room temperature. Subsequently, 2,7-dibromobiphenyleno[1,2-*b*:5,6-*b*′]dithiophene (**13**, 66.7 mg, 0.158 mmol) and Pd(dppf)Cl_2 (5.0 mg, 6.8 μmol, 4.3 mol%) were added. The resulting mixture was stirred at room temperature for 5 h. After addition of 1 N HCl to the ice-cold mixture, the mixture was extracted with toluene, washed with water, dried over Na_2SO_4, and concentrated *in vacuo*. The residue was purified by column chromatography on silica gel (hexane) followed by recrystallization from hexane to give 2,7-dioctylbiphenyleno[1,2-*b*:5,6-*b*′] dithiophene (**C8-B2-BPDT**, 35.2 mg, 0.072 mmol, 46%) as yellow needles. Mp 107.3–108.5 °C; ^{1}H NMR (400 MHz, $CDCl_3$): δ 0.89 (t, J = 6.4 Hz, 6H), 1.25–1.40 (m, 20H), 1.70 (m, 4H), 2.78 (t, J = 7.4 Hz, 4H), 6.63 (d, J = 7.3 Hz, 2H), 6.69 (s, 2H), 6.99 (d, J = 7.0 Hz, 2H); ^{13}C NMR (100 MHz, $CDCl_3$): δ 14.28, 22.83, 29.26, 29.37, 29.50, 30.77, 31.12, 32.02, 114.08, 120.99, 121.50, 127.93, 143.61, 144.95, 145.60, 147.44; TOF HRMS (APCI): calcd for $C_{32}H_{41}S_2$ $[M + H]^+$ 489.2644, found, 489.2630.

2,6-Dibromo-3,7-difluorobiphenylene (14). To a solution of **4** (314 mg, 1.67 mmol) in DMF (8 mL) was added NBS (986 mg, 5.54 mmol) and the resulting mixture was stirred for 10 h at 40 °C. After addition of water at room temperature, the resulting mixture was extracted with toluene, washed with water, dried over Na_2SO_4, and concentrated *in vacuo*. The residue was purified by recrystallization from toluene : heptane (1 : 1) to afford 2,6-dibromo-3,7-difluorobiphenylene (**14**, 353 mg, 1.02 mmol, 61%) as pale yellow needles. Mp 230.1–231.0 °C; ^{1}H NMR (400 MHz, $CDCl_3$): δ 6.49 (d, J = 6.5 Hz, 2H), 6.82 (d, J = 5.7 Hz, 2H); ^{13}C NMR (100 MHz, $CDCl_3$): δ 107.42 (d, J = 24.1 Hz, C_{quat}), 109.31 (d, J = 28.1 Hz, CH), 123.44 (CH), 144.12 (C_{quat}), 150.33 (d, J = 6.6 Hz, C_{quat}), 159.94 (d, J = 250.0 Hz, C_{quat}).

2,6-Di(dec-1-yn-1-yl)-3,7-difluorobiphenylene (15). 1-Decyne (458 mg, 3.31 mmol) was added to a solution of **14** (179 mg, 0.517 mmol), triethylamine (5.5 mL), $Pd(PPh_3)_2Cl_2$ (33.7 mg, 0.0480 mmol, 9.3 mol%), and CuI (18.8 mg, 0.0987 mmol, 19.1 mol%) in toluene (3.5 mL). After the mixture was stirred for 50 h at 60 °C, water was added at room temperature. The resulting mixture was extracted with toluene, washed with water, dried over Na_2SO_4, and concentrated *in vacuo*. The residue was purified by column chromatography on silica gel eluting with hexane to give 2,6-di(dec-1-yn-1-yl)-3,7-difluorobiphenylene (**15**, 222 mg, 0.481 mmol, 93%) as a pale yellow solid. Mp 78.2–78.9 °C; ^{1}H NMR (400 MHz, $CDCl_3$): δ 0.89 (t, J = 7.2 Hz, 6H), 1.31 (m, 16H), 1.43 (m, 4H), 1.61 (m, 4H), 2.42 (t, J = 7.1 Hz, 4H), 6.42 (d, J = 7.4 Hz, 2H), 6.60 (d, J = 5.7 Hz, 2H); ^{13}C NMR (100 MHz, $CDCl_3$): δ 14.28, 19.86, 22.83, 28.75, 29.02, 29.25, 29.35, 31.99, 74.27 (C_{quat}), 97.18 (C_{quat}), 108.07 (d, J = 27.3 Hz, C_{quat}), 110.49 (d, J = 19.5 Hz, CH), 122.10 (CH), 142.90 (C_{quat}), 150.71 (d, J = 7.5 Hz, C_{quat}), 164.57 (d, J = 252.9 Hz, C_{quat}).

2,7-Dioctylbiphenyleno[2,3-*b*:6,7-*b*′]dithiophene (C8-L-BPDT). NMP (3 mL) was added to a mixture of **15** (93.7 mg, 0.199 mmol) and sodium sulfide nonahydrate (164 mg, 0.684 mmol) and then the resulting mixture was heated at 80 °C for 3 h. After cooling, water was added and the resulting precipitate was collected by filtration. The precipitate was washed sequentially with water, methanol and toluene, purified by column chromatography on silica gel (toluene), and then recrystallized from toluene to give 2,7-dioctylbiphenyleno[2,3-*b*:6,7-*b*′]dithiophene (**C8-L-BPDT**, 59.8 mg, 0.122 mmol, 61%) as a red solid. Mp 284.3–285.1 °C; ^{1}H NMR (400 MHz, $CDCl_3$, 55 °C): δ 0.90 (t, J = 6.9 Hz, 6H), 1.20–1.45 (m, 20H), 1.72 (m, 4H), 2.82 (t, J = 7.4 Hz, 4H), 6.78 (s, 2H), 6.94 (s, 2H), 7.03 (s, 2H); ^{13}C NMR (100 MHz, $CDCl_3$, 55 °C): δ 14.17, 22.82, 29.33, 29.37, 29.52, 30.83, 31.37, 32.05, 111.86, 112.34, 121.86, 138.78, 139.56, 145.43, 145.84, 146.35; TOF HRMS (APCI): calcd for $C_{32}H_{41}S_2$ $[M + H]^+$ 489.2644, found, 489.2626.

Characterization of compounds

Solubilities. The solubility of **C8-B1-BPDT** was estimated using the following method. A solution of **C8-B1-BPDT** (1.0 wt%) in toluene at 23 °C was prepared and then the solvent

was gradually evaporated at 23 °C. The concentration was determined by microscope inspection before observing precipitation. The solubilities of **C8-B2-BPDT** and **C8-L-BPDT** were estimated by adding toluene until complete dissolution was obtained at 23 °C.

Single-crystal analyses. Recrystallization from heptane gave single crystals of **C8-B1-BPDT** and **C8-B2-BPDT** suitable for X-ray crystallographic analysis. X-ray crystallographic analysis was conducted on a Rigaku XtaLAB Synergy, Dualflex, HyPix diffractometer (Cu Kα radiation, λ = 1.54184 Å, T = 100 K). Each structure was solved and its space group determined by the ShelXT 2018/2 (Sheldrick, 2018) structure solution program using intrinsic phasing and refined by least squares using version 2018/3 of ShelXL 2018/3 (Sheldrick, 2015). All non-hydrogen atoms were refined anisotropically. Hydrogen-atom positions were calculated geometrically and refined using the riding model.

Physicochemical properties. Laser microscope images were observed using a Lasertec hybrid laser microscope. SEM images were obtained by using a JSM-7100F (JEOL Ltd.). AFM images were obtained by using an E-sweep (Hitachi High-Tech Science Corporation). UV–vis absorption spectra were recorded in air using a JASCO V-770 spectrometer. UV–vis spectra were measured in dichloromethane (concentration: 10^{-5}–10^{-6} M) or as thin films on a parylene-C layer. The bulk structure of thin films was evaluated by out-of-plane and in-plane XRD measurements using a Rigaku Smart-Lab diffractometer. Ionization energies were measured on a Riken Keiki AC-5 photoelectron spectrometer. DSC was carried out on a Hitachi DSC7000X. XRD data for the thin films on a parylene-C layer were obtained with a CuKα source (λ = 1.541 Å) in air. IPs were determined by photoemission yield spectroscopy in air. Laser microscope images of the thin films were obtained in air.

Fabrication and evaluation of OTFTs. OTFTs with a bottom-gate-bottom-contact configuration were fabricated on glass substrates. On each substrate, a silver film (50 nm) as a gate electrode was vacuum deposited through a shadow mask. A parylene-C (Kisco, diX-C) gate dielectric layer (450 nm, C_i = 6.29 nF cm^{-2}) was fabricated by chemical vapor deposition using dichloro-di-*p*-xylylene as a starting material. On top of the gate dielectric film, gold films (50 nm) as drain and source electrodes were vacuum deposited through a shadow mask. The drain–source channel length (L) and width (W) were 100 and 500 μm, respectively. Next, a self-assembled monolayer was formed on the source and drain electrodes by immersing the substrates in a solution of pentafluorobenzenethiol (30×10^{-3} mol L^{-1}) in propanol for 5 min at room temperature. The substrates were rinsed with propanol and dried with nitrogen. **C8-B1-BPDT** and **C8-B2-BPDT** were dissolved in toluene with a concentration of 2 mg mL^{-1}. The solutions were drop cast on the substrates at 23 °C. After 30 min of natural drying, the resulting films were annealed for 30 min at 80 °C to remove any residue solvent. The film thickness was around 45–55 nm. After formation of a self-assembled monolayer on the source and drain electrodes at room temperature, a thin film of **C8-L-BPDT** (75 nm) as the active layer was vacuum-deposited on the parylene-C dielectric layer at a rate of 0.2 Å s^{-1} under a pressure of ~10^{-6} Pa. Characteristics of the OTFT devices were measured at room temperature in air with a Keithley 4200-SCS semiconductor parameter analyzer. Field-effect mobility (μ_{FET}) was calculated in the saturation regime (V_d = −20 V) of the drain current (I_d) using the following equation:

$$I_d = (WC_i/2L)\mu_{FET}(V_g - V_{th})^2, \quad (1)$$

where C_i is the capacitance of the parylene-C insulator, and V_g and V_{th} are the gate and threshold voltages, respectively. The current on/off ratio (I_{on}/I_{off}) was determined from I_d at V_g = 0 V (I_{off}) and V_g = −20 V (I_{on}).

Interface trap density (D_{it}) was estimated from the values of subthreshold swing (SS) in the transfer characteristics using the following equation:[36]

$$SS = (kT/q)\ln 10(1 + q^2 D_{it}/C_i) \quad (2)$$

where k is the Boltzmann constant, T is the temperature in kelvin, q is the electronic charge and C_i is the capacitance of the dielectric.

Author contributions

M. Watanabe: synthesis and characterization of synthetic products, writing the manuscript. M. Miyashita: synthesis and characterization of synthetic products. T. Fukuda and S. Oku: OTFT device fabrication, electric data analysis.

Conflicts of interest

There are no conflicts to declare.

Data availability

The data supporting this article have been included as part of the supplementary information (SI).

Supplementary information including NMR spectra of products is available. See DOI: https://doi.org/10.1039/d5ce01050k.

CCDC 2477388 (**C8-B1-BPDT**) and 2477349 (**C8-B2-BPDT**) contain the supplementary crystallographic data for this paper.[37a,b]

Acknowledgements

We thank Dr R. Tanaka (Sagami Chemical Research Institute) for measurement and analysis of single-crystal X-ray crystallography data.

Notes and references

1 J. E. Anthony, *Chem. Rev.*, 2006, **106**, 5028–5048.
2 H. Ebata, T. Izawa, E. Miyazaki, K. Takimiya, M. Ikeda, H. Kuwabara and T. Yui, *J. Am. Chem. Soc.*, 2007, **129**, 15732–15733.

3 S. Shinamura, I. Osaka, E. Miyazaki, A. Nakao, M. Yamagishi, J. Takeya and K. Takimiya, *J. Am. Chem. Soc.*, 2011, **133**, 5024–5035.
4 K. Takimiya, S. Shinamura, I. Osaka and E. Miyazaki, *Adv. Mater.*, 2011, **23**, 4347–4370.
5 M. Nakano, K. Niimi, E. Miyazaki, I. Osaka and K. Takimiya, *J. Org. Chem.*, 2012, **77**, 8099–8111.
6 P. Gao, D. Beckmann, H. N. Tsao, X. Feng, V. Enkelmann, M. Baumgarten, W. Pisula and K. Müllen, *Adv. Mater.*, 2009, **21**, 213–216.
7 T. Okamoto, C. Mitsui, M. Yamagishi, K. Nakahara, J. Soeda, Y. Hirose, K. Miwa, H. Sato, A. Yamano, T. Matsushita, T. Uemura and J. Takeya, *Adv. Mater.*, 2013, **25**, 6392–6397.
8 C. Mitsui, T. Okamoto, M. Yamagishi, J. Tsurumi, K. Yoshimoto, K. Nakahara, J. Soeda, Y. Hirose, H. Sato, A. Yamano, T. Uemura and J. Takeya, *Adv. Mater.*, 2014, **26**, 4546–4551.
9 K. Fukuda, T. Minamiki, T. Minami, M. Watanabe, T. Fukuda, D. Kumaki and S. Tokito, *Adv. Electron. Mater.*, 2015, **1**, 1400052.
10 H. Iino, T. Usui and J. Hanna, *Nat. Commun.*, 2015, **6**, 6828.
11 S. Inoue, T. Higashino, S. Arai, R. Kumai, H. Matsui, S. Tsuzuki, S. Horiuchi and T. Hasegawa, *Chem. Sci.*, 2020, **11**, 12493–12505.
12 T. Higashino, S. Inoue, S. Arai, H. Matsui, N. Toda, S. Horiuchi, R. Azumi and T. Hasegawa, *Chem. Mater.*, 2021, **33**, 7379–7385.
13 S. Allard, M. Forster, B. Souharce, H. Thiem and U. Scherf, *Angew. Chem., Int. Ed.*, 2008, **47**, 4070–4098.
14 N. S. Yusof, M. F. P. Mohamed, N. A. Ghazali, M. F. A. J. Khan, S. Shaari and M. N. Mohtar, *Alexandria Eng. J.*, 2022, **61**, 11405–11431.
15 H. Takano, T. Ito, K. S. Kanyiva and T. Shibata, *Eur. J. Org. Chem.*, 2019, 2871–2883.
16 D. N. Nicolaides, *Synthesis*, 1977, 127–129.
17 A. Fukazawa, H. Oshima, Y. Shiota, S. Takahashi, K. Yoshizawa and S. Yamaguchi, *J. Am. Chem. Soc.*, 2013, **135**, 1731–1734.
18 V. G. Wittig and G. Klar, *Liebigs Ann. Chem.*, 1967, **704**, 91–108.
19 P. I. Dosa, Z. Gu, D. Hager, W. L. Karney and K. P. C. Vollhardt, *Chem. Commun.*, 2009, 1967–1969.
20 T. Kashiki, S. Shinamura, M. Kohara, E. Miyazaki, K. Takimiya, M. Ikeda and H. Kuwabara, *Org. Lett.*, 2009, **11**, 2473–2475.
21 Y. Li, L. Cheng, B. Li, S. Jiang, L. Chen and Y. Shao, *ChemistrySelect*, 2016, **1**, 1092–1095.
22 F. R. Leroux, L. Bonnafoux, C. Heiss, F. Colobert and D. A. Lanfranchi, *Adv. Synth. Catal.*, 2007, **349**, 2705–2713.
23 S. L. Wang, M. L. Pan, W. S. Su and Y. T. Wu, *Angew. Chem., Int. Ed.*, 2017, **56**, 14694–14697.
24 P. A. Ple and L. Marnett, *J. Heterocyclic Chem.*, 1988, **25**, 1271–1272.
25 H. Y. Chen, G. Schweicher, M. Planells, S. M. Ryno, K. Boch, A. J. P. White, D. Simatos, M. Little, C. Jellett, S. J. Cryer, A. Marks, M. Hurhangee, J. L. Bredas, H. Sirringhaus and I. McCulloch, *Chem. Mater.*, 2018, **30**, 7587–7592.
26 J. Smith, R. Hamilton, I. McCulloch, N. Stingelin-Stutzmann, M. Heeney, D. D. C. Bradley and T. D. Anthopoulos, *J. Mater. Chem.*, 2010, **20**, 2562–2574.
27 S. Shinamura, E. Miyazaki and K. Takimiya, *J. Org. Chem.*, 2010, **75**, 1228–1234.
28 A. Pietrangelo, M. J. MacLachlan, M. O. Wolf and B. O. Patrick, *Org. Lett.*, 2007, **9**, 3571–3573.
29 A. Pietrangelo, B. O. Patrick, M. J. MacLachlan and M. O. Wolf, *J. Org. Chem.*, 2009, **74**, 4918–4926.
30 B. Tylleman, C. M. L. V. Velde, J. Y. Balandier, S. Stas, S. Sergeyev and Y. H. Geerts, *Org. Lett.*, 2011, **13**, 5208–5211.
31 M. Mamada, T. Minamiki, H. Katagiri and S. Tokito, *Org. Lett.*, 2012, **14**, 4062–4065.
32 Y. Yi, L. Zhu and J. L. Brédas, *J. Phys. Chem. C*, 2012, **116**, 5215–5224.
33 C. Quinton, M. Suzuki, Y. Kaneshige, Y. Tatenaka, C. Katagiri, Y. Yamaguchi, D. Kuzuhara, N. Aratani, K. Nakayama and H. Yamada, *J. Mater. Chem. C*, 2015, **3**, 5995–6005.
34 J. G. Laquindanum, H. E. Katz and A. J. Lovinger, *J. Am. Chem. Soc.*, 1998, **120**, 664–672.
35 W. L. Liau, T. H. Lee, J. T. Chen and C. S. Hsu, *J. Mater. Chem. C*, 2016, **4**, 2284–2288.
36 M. Yoon, K. R. Ko, S. W. Min and S. Im, *RSC Adv.*, 2018, **8**, 2837–2843.
37 (*a*) CCDC 2477388: Experimental Crystal Structure Determination, 2025, DOI: 10.5517/ccdc.csd.cc2p4xrj; (*b*) CCDC 2477349: Experimental Crystal Structure Determination, 2025, DOI: 10.5517/ccdc.csd.cc2p4wh7.